

REVIEW

Quantitative approaches of dynamic FDG-PET and PET/CT studies (dPET/CT) for the evaluation of oncological patients

Antonia Dimitrakopoulou-Strauss, Leyun Pan, Ludwig G. Strauss

*Medical PET Group – Biological Imaging, Clinical Cooperation Unit Nuclear Medicine,
German Cancer Research Center, Heidelberg, Germany*

*Corresponding address: Antonia Dimitrakopoulou-Strauss, Medical PET Group – Biological Imaging (E0601),
Clinical Cooperation Unit Nuclear Medicine, German Cancer Research Center, Im Neuenheimer Feld 280,
D-69120 Heidelberg, Germany.*

Email: a.dimitrakopoulou-strauss@dkfz.de

Date accepted for publication 9 June 2012

Abstract

Objectives: The use of dynamic positron emission tomography/computed tomography (dPET/CT) studies with [^{18}F]deoxyglucose (FDG) in oncological patients is limited and primarily confined to research protocols. A more widespread application is, however, desirable, and may help to assess small therapeutic effects early after therapy as well as to differentiate borderline differences between tumour and non-tumour lesions, e.g., lipomas versus low-grade liposarcomas. The aim is to present quantification approaches that can be used for the evaluation of dPET/CT series in combination with parametric imaging and to demonstrate the feasibility with regard to tumour diagnostics and therapy management. **Methods:** A 60-min data acquisition and short acquisition protocols (20-min dynamic series and a static image 60 min post injection) are discussed. A combination of a modified two-tissue compartment model and non-compartmental approaches from the chaos theory (fractal dimension of the time–activity curves) are presented. Fused PET/CT images as well as regression-based parametric images fused with CT or with PET/standardised uptake value images are demonstrated for the exact placement of volumes of interest. **Results:** The two-tissue compartmental method results in the calculation of 5 kinetic parameters, the fractional blood volume V_B (known also as the distribution volume), and the transport rates k_1 to k_4 . Furthermore, the influx according to Patlak can be calculated from the transport rates. The fractal dimension of the time–activity curves describes the heterogeneity of the tracer distribution. The use of the regression-based parametric images of FDG helps to visualise the transport/perfusion and the transport/phosphorylation-dependent FDG uptake, and adds a new dimension to the existing conventional PET or PET/CT images. **Conclusions:** More sophisticated quantification methods and dedicated software as well as high computational power and faster acquisition protocols can facilitate the assessment of dPET/CT, and may find use in clinical routine, in particular for the assessment of early therapeutic effects or new treatment protocols in combination with the new generation of PET/CT scanners.

Keywords: *Dynamic PET; oncology; compartment modelling; non-compartment modelling; parametric imaging; feature extraction.*

Rationale for dynamic PET and PET/CT

Positron emission tomography (PET) and PET/computed tomography (CT) are used in oncological patients for primary diagnostics, staging and therapy monitoring. The application of dynamic imaging with PET (dPET) or PET/CT (dPET/CT) is confined to research projects for

scientific purposes because it is more time consuming and requires dedicated evaluation software. However, the introduction of a new generation of PET/CT scanners with, for example, new detector material such as lutetium oxyorthosilicate (LSO), which provides an improved count rate performance, as well as the three-dimensional acquisition protocols, reduces the total acquisition time. The improvement in computer power, the introduction

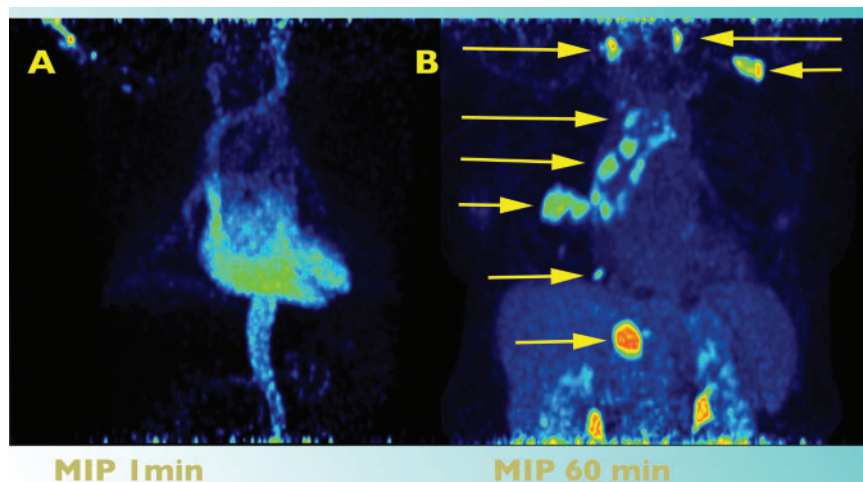


Figure 1 Maximum-intensity projection (MIP) images 1 min (A) and 55–60 min (B) after intravenous FDG injection in a patient with a metastatic lung tumour in the right lung, multiple mediastinal lymph node metastases at both sides, and intrapulmonary and liver metastases. The early MIP image clearly demonstrates the blood activity in the heart and the large arterial vessels over two bed positions (field of view: 43.2 cm).

of new-generation PET/CT scanners, and the development of more sophisticated software for data analysis are facilitating a more widespread application of dPET or dPET/CT also within clinical environments.

Dynamic imaging allows the registration of the tracer kinetics over time, not only at one time point after the tracer injection in the manner of static images. Pharmacokinetic studies are helpful not only for the evaluation of new tracers but also for the evaluation of small therapeutic effects, for example, using [^{18}F]fluorodeoxyglucose (FDG) early after the onset of chemotherapy. Furthermore, the use of kinetic parameters may help to differentiate between benign and less aggressive tumours (e.g. lipomas from low-grade liposarcomas)^[1].

Based on dynamic data sets, parametric imaging can be applied using different algorithms. Parametric images allow the visualization of dedicated parameters of the radiopharmaceutical's kinetics, such as perfusion, transport or phosphorylation in the case of FDG. A fast and robust method is the regression-based calculation of parametric images, which results in slope and intercept images^[2,3]. In particular for FDG, the calculation of regression-based parametric images of the slope, which are related to the transport/phosphorylation-dependent part of FDG, may facilitate diagnostics by delineating small lesions with high contrast, which are not clearly seen in conventional images because of the high amount of FDG in the surrounding tissue and/or a high fractional blood volume in the target area. Furthermore, regression-based parametric images of the intercept, which are related to the transport/perfusion-dependent part of FDG, may be helpful in delineating metastatic lesions that are not FDG avid, for example because of several chemotherapeutic treatments or because they may be

cystoid, as in patients with gastrointestinal stromal tumours (GIST)^[4].

We present methods for the quantification of dynamic PET and PET/CT studies within oncology.

dPET and dPET/CT studies

dPET studies at our institution are performed over the target area, which is mostly the primary, recurrent or metastatic tumour, for 60 min following the intravenous application of FDG using a 28-frame protocol (10 frames of 30 s, 5 frames of 60 s, 5 frames of 120 s and 8 frames of 300 s). A software update allows the dynamic acquisition over multiple bed positions. This option provides the possibility of acquisition over multiple bed positions using the list mode protocol. The defined frames are divided by the number of bed positions acquired (e.g. 2), and the bed moves during each frame. The frequency of the movement is dependent on the number of bed positions acquired. In the case of 2 bed positions, the bed moves up and down during one frame. An example of a dynamic acquisition over 2 bed positions is presented in Fig. 1. Additional static images are acquired in all patients to cover a larger area for diagnostic purposes. A dedicated PET/CT system (Biograph mCT S128, Siemens Co., Erlangen, Germany) with an axial field of view of 21.6 cm with TrueV, operated in a three-dimensional mode, is used for patient studies. The system allows the simultaneous acquisition of 56 transversal slices (1 bed position) with a theoretical slice thickness of $2.036 \times 2.036 \times 4$ mm. A low-dose attenuation CT (80 kV, 30 mA) is used for the attenuation correction of the dynamic emission PET data and for image fusion. All PET images are attenuation corrected and an image matrix of 400×400 pixels is used for iterative image

reconstruction. The reconstructed images are converted to standardized uptake value (SUV) images^[5].

The calculation of the parametric images and the evaluation of the dPET data are performed using the software package PMOD (PMOD Technologies Ltd., Zürich, Switzerland)^[6]. Visual analysis of the static PET/CT images is performed by evaluating the hypermetabolic areas on transaxial, coronal and sagittal images by two experienced nuclear medicine physicians (A.D.S., L.G.S.) using an Aycan workstation Osirix pro 2.0 (Aycan Digitalsysteme GmbH, Würzburg, Germany).

Approaches for quantitative evaluation

SUV

The calculation of average and maximum SUV is performed according to the formula: $\text{SUV} = \text{tissue concentration (Bq/g)} / (\text{injected dose (Bq)} / \text{body weight (g)})$ using volumes of interest (VOIs) over the target area, which is mostly the tumour as well as reference tissue for comparison. We apply a 50% isocontour for the VOI definition.

Two-tissue compartment model

This model is appropriate for tracers, which are transported and, after the first metabolic step, trapped, as in the case of FDG. A two-tissue compartment model first described by Sokoloff et al.^[11] was used for the quantification of brain studies. Four transport rates (k_1 , k_2 , k_3 , k_4) describe the exchange of the tracer between blood and tissue. In the case of FDG, k_1 reflects the influx, k_2 the efflux, k_3 the phosphorylation rate and k_4 the dephosphorylation rate of the glucose analogue. A simplification of the model consists of the summary of the interstitial and cellular space. A modification of the two-tissue compartment model consists of the calculation of the fractional blood volume, which is a parameter that correlates to the blood volume and is called V_B (also known as vessel density). This model is different to that proposed by Sokoloff et al., which does not take k_4 and V_B into account. The lack of k_4 and V_B of the model proposed by Sokoloff et al. leads to different k_1 and k_3 values, since k_1 is dependent on V_B and k_3 on k_4 . The dephosphorylation rate (k_4) of FDG was low in all these oncological studies, but not negligible^[11]. Details about the applied compartment model are described by Burger and Buck^[7]. Details about the use of the two-tissue compartment model in oncological patients performed at our institution has been described elsewhere in detail^[2,3]. The model parameters were accepted when V_B and k_1 to k_4 were less than 1 and the V_B values exceeded 0. The unit for the rate constants k_1 to k_4 is 1/min, while V_B reflects the fraction of blood within the evaluated volume.

Influx based on Patlak

A prerequisite for the use of a Patlak plot is an irreversible trapping compartment of the tracer, as in the case of FDG^[8]. The model demonstrates whether the major metabolic step fits with a unidirectional transfer of the tracer. If this assumption is valid, an influx constant (K_i) can be calculated graphically. The model is based on a blood/plasma compartment, a reversible and a non-reversible compartment.

The influx rate K_i presents the slope of the time–activity curve, which is linear if the metabolic step of a tracer is irreversible. The intercept in the y axis correlates to the fractional blood volume (V_B). The metabolic rate of FDG (MRFDG) can then be calculated using the formula: $\text{MRFDG} = K_i \times (\text{plasma glucose/lumped constant})$. The lumped constant indicates the ratio of FDG uptake to glucose uptake and is not exactly known for the tumours. Therefore, a value of 1 is used in tumours as an estimate.

If a two-tissue compartment is fitted to the data, the influx rate can also be calculated using the rate constants of the two-tissue compartment and the formula: $K_i = (k_1 \times k_3 / k_2 + k_3)$.

Input function

The accurate measurement of the input function theoretically requires arterial blood sampling. However, the input function can be retrieved from the image data with good accuracy^[9]. For the input function, the mean value of the VOI data obtained from a large arterial vessel is used. A vessel VOI consists of at least 10 regions of interest (ROIs) in sequential PET images. The recovery coefficient is 0.85 for a diameter of 8 mm and for the system described above. Partial volume correction was performed in selected cases for small vessels or lesions (diameter <8 mm) on the basis of phantom measurements of the recovery function using the PMOD software. Noise in the input curve has an effect on the parameter estimates. Therefore we used a pre-processing tool, available in the PMOD software, which allows a fit of the input curve, namely by a sum of up to 3 decaying exponentials, to reduce noise^[6,7].

Fractal dimension

Non-compartment models can also be used for the evaluation of dynamic PET or PET/CT data sets. We applied a model based on the fractal dimension for the quantification of the time–activity curves. The fractal dimension (FD) is a parameter for the heterogeneity and was calculated for the time–activity data in each individual voxel of a VOI. The values of the FD vary from 0 to 2, showing the deterministic or chaotic distribution of the tracer activity. We used a subdivision of 7×7 (this means that each time activity is handled like an image and is divided by a matrix of 7×7 squares) and a maximal SUV of 20 for the calculation of FD^[12]. Furthermore, we calculated parametric images of the FD. The example

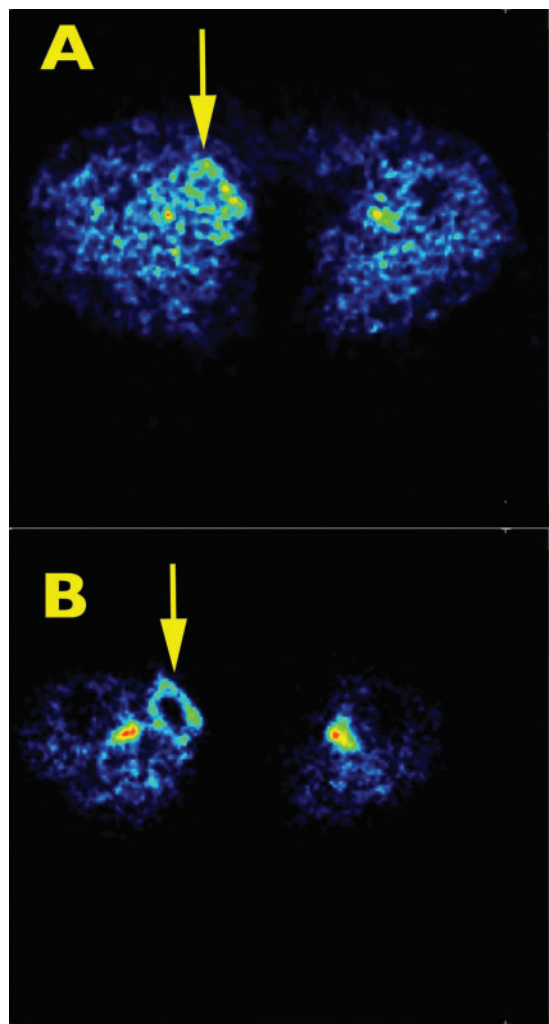


Figure 2 Transversal slice of the upper legs 55–60 min after FDG injection. (A) Moderate enhanced FDG uptake in the medial parts of the soft-tissue tumour. (B) Parametric image of the fractal dimension revealing a clearly enhanced signal, in particular in the peripheral parts of the tumour, as well as in the vessels of the upper leg. Enhanced fractal dimension is related to tumour heterogeneity. Vessels are shown with a positive signal due to the enhanced fractal dimension of the blood.

in Fig. 2 demonstrates an enhancement of the FD within the peripheral parts of a soft-tissue tumour of the upper leg on the parametric image of the FD, which indicates enhanced heterogeneity in this part of the tumour.

Parametric imaging

Regression-based analysis

Parametric images were calculated based on the dPET or dPET/CT data by fitting a linear regression function to the time–activity data and for each pixel. Images of the slope and the intercept of the time–activity data can be

calculated using the PMOD software. Parametric images of the slope reflect primarily the trapping of FDG and may be used for the delineation of the malignant lesions and the VOI's placement due to the high contrast in the surrounding tissue. Parametric images of the intercept reflect the distribution volume of FDG, and may be used for better anatomic localization of the lesions due to delineation of the vessels. Details of this method have been described elsewhere^[2]. Parametric images of the distribution volume have been used for better anatomic delineation of the vessels and in some tumours with low FDG uptake for better delineation of the tumour (e.g. in desmoids^[3]).

Fig. 3 demonstrates an example of a patient with liver metastases from a GIST after several chemotherapeutic cycles. The FDG SUV image (55–60 min post injection) clearly demonstrates a decrease in the FDG uptake in a liver metastasis in the ventral part of the right liver lobe. Interestingly, viability was shown in the regression-based slope images, which are related to the phosphorylation, only in a small area of this metastasis located in the ventrolateral part of the lesion. The other parts of this metastatic lesion do not demonstrate enhanced phosphorylation. The regression-based intercept images, which are related to the blood volume, show a low distribution volume of the FDG in the liver metastasis. Restaging data confirmed this result. Fig. 4 shows another example of a liver metastasis secondary to GIST, after selective internal radiotherapy treatment (SIRT). This metastasis is hypodense on CT and demonstrates a low distribution volume in the parametric intercept image, but shows a high homogeneous enhanced signal in the parametric slope images, which is associated with enhanced phosphorylation.

Short acquisition protocols

One possibility that may facilitate the use of dynamic imaging within clinical routine consists in the use of shorter acquisition protocols, not longer than 30 min. We evaluated the results of the two-tissue compartment model using 60-min acquisition as well as different shorter acquisition protocols. The results were based on 1474 time–activity curves from 539 patients in whom dynamic FDG studies were performed. We used dedicated software that is based on a modified support vector machines (SVM) algorithm and predicts the data of the two-tissue compartment model. We found that either a dynamic series of 16 min or a combination of a dynamic PET or PET/CT series of 20 min and a 60-min uptake image is accurate for the prediction of the kinetic parameters^[13].

Discussion

The major advantage of PET or PET/CT is the quantitative aspect, which is not taken into consideration when

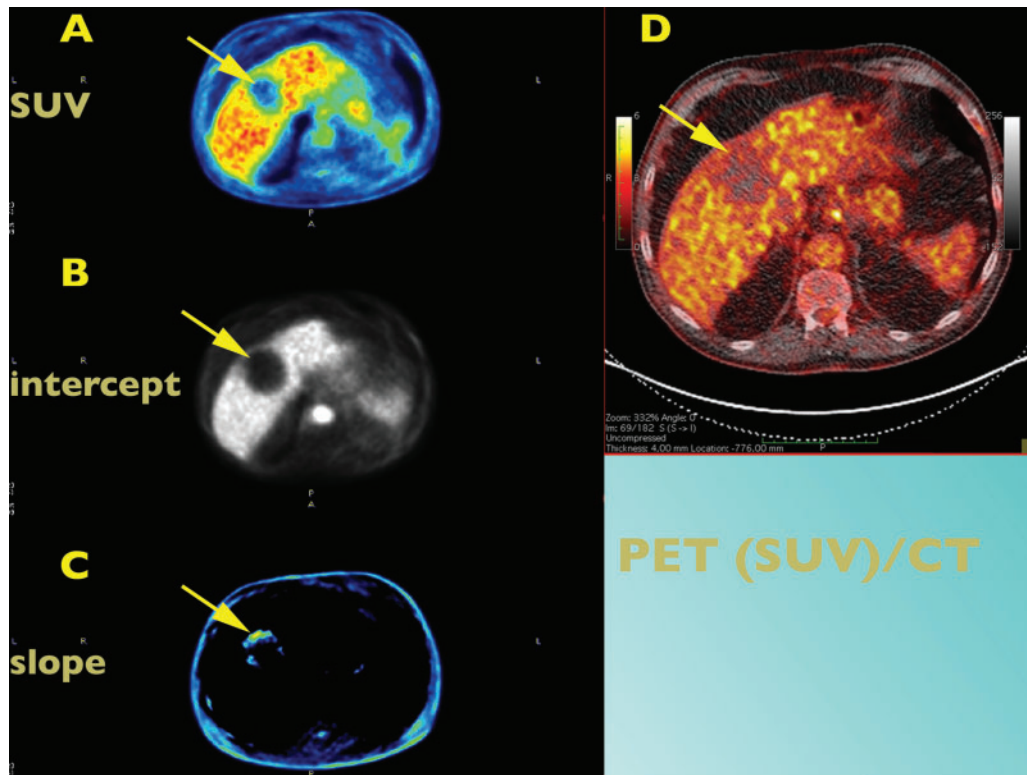


Figure 3 FDG PET/CT study in a patient with liver metastases from GIST following several treatments of imatinib for therapy monitoring. (A) 55–60 min SUV image of the liver demonstrating a decreased uptake in a liver metastasis in the ventral part of the right liver lobe. (B) Parametric image of the intercept (related to blood volume) showing also a decrease of blood volume in the liver metastasis. (C) Parametric image of the slope (related to phosphorylation) demonstrating an enhanced phosphorylation only in the ventral part of the liver metastasis. (D) Fused FDG (SUV) and CT images. The metastasis is hypodense on CT.

using only whole-body protocols and visual evaluation as a primary diagnostic tool in oncological patients. Semiquantitative data evaluation based, e.g., on the calculation of SUVs is often performed, at least for therapy monitoring purposes. To gain more quantitative data, the use of dynamic scanning is needed. This approach is more time consuming but has the major advantage of full utilisation of the PET or PET/CT technique^[10]. dPET provides the possibility of absolute data quantification based on compartment and non-compartment methods and, furthermore, allows the calculation of parametric images. New acquisition protocols provided by the manufacturers allow dynamic imaging over more than one bed position. This is a major step forward because it allows the dynamic examination of a larger area (partial body dynamic scanning) and is not restricted to one organ, as occurred in the past.

Parametric images are a method of feature extraction. Based on dedicated algorithms it is possible to visualise one isolated parameter of the tracer kinetics. In the case of FDG, the idea is to visualise only the perfusion-dependent part of the tracer or only the phosphorylated part. For the calculation of parametric images, different

methods are available with specific advantages and limitations. An advantage for the users, in particular within a clinical environment, is the lack of any data pre-processing, such as the definition of an input VOI. One robust and operator-friendly method consists in the calculation of regression-based images of the intercept and the slope. Intercept images reflect primarily the perfusion-dependent part of FDG, whereas slope images are related to the phosphorylated part of FDG. Figs. 3 and 4 demonstrate representative examples of this approach. Slope images may be helpful especially in patients with several chemotherapeutic treatments and a relatively low global FDG uptake, in terms of SUV. An enhanced slope may indicate residual viable tumour tissue, even when the SUV images do not show an enhancement, as in treated liver metastases. Lesions with a positive slope and low SUVs should be treated carefully and closely monitored, because of the higher possibility of residual tumour tissue.

The classical approach is the use of a two-tissue compartment model for the calculation of parametric images of the vessel density (V_B) and the transport rates k_1 to k_3 . However, this method does not function for the

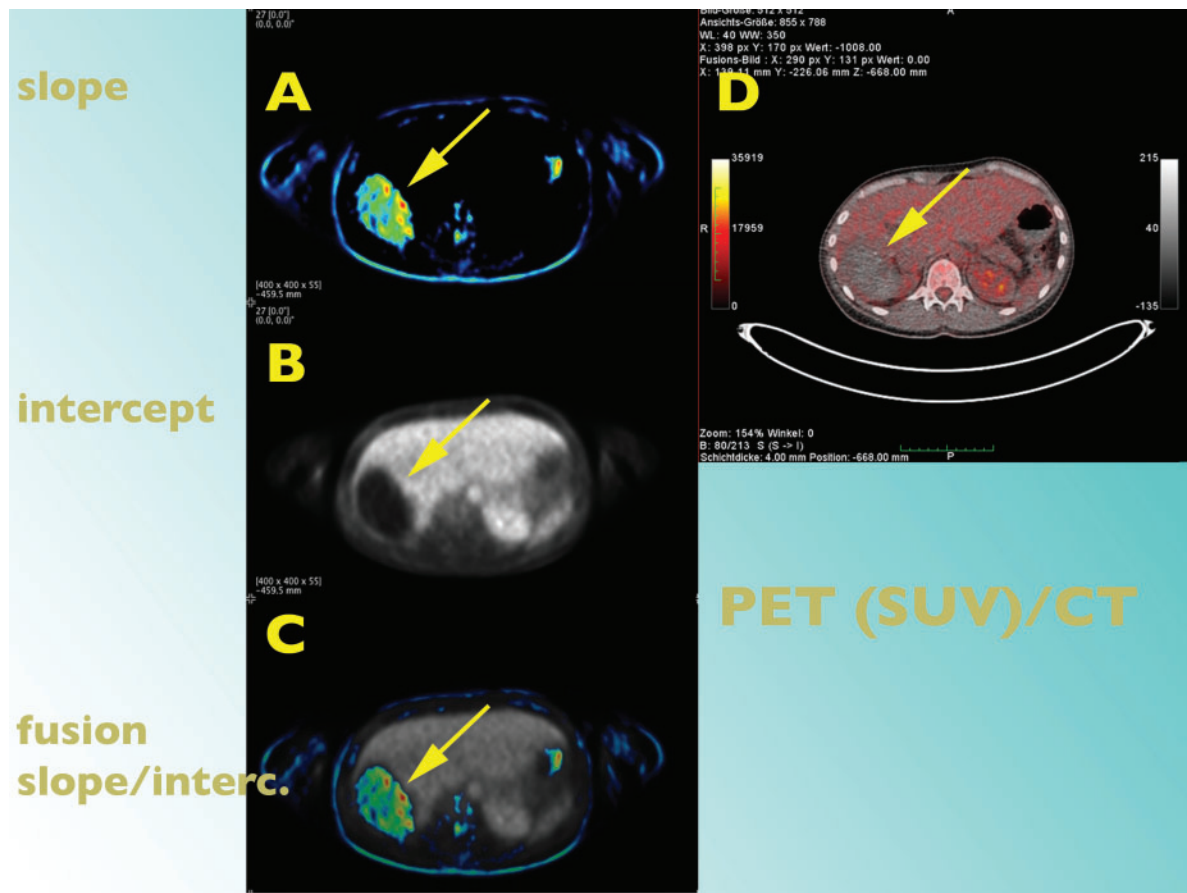


Figure 4 FDG PET/CT study in another patient with a large liver metastasis secondary to GIST following selective internal radiotherapy treatment (SIRT) therapy. The fused FDG PET/CT images show a low FDG uptake in the hypodense lesion (D). The parametric images, however, demonstrate a low distribution volume in the intercept images (B) but a high signal in the slope images (A), indicating a high phosphorylation of the tracer. (C) Fused images of slope and intercept.

calculation of pixel-wise parametric images. The reason for this is that compartment models traditionally use an iterative fitting (IF) method to find the least squares between the measured and calculated values over time, which may encounter some problems such as overfitting of model parameters and lack of reproducibility. Therefore, we introduced a machine learning (ML)-based kinetic modelling (KM) method, which can utilise a reference database to build a moderate kinetic model directly dealing with noisy data but not trying to smooth the noises in the image. Details on this method are described elsewhere^[14].

Patlak graphical analysis is another approach suitable for the calculation of the metabolic rate of glucose. However, this method requires an input function and a lumped constant that indicates the ratio of FDG uptake to glucose uptake, and is not precisely known for the tumours. Therefore, a value of 1 is used in tumours as an estimate. Messa et al. reported on the use of parametric Patlak images in patients with liver metastases in 1992^[15]. They stated that uncorrected Patlak graphical

analysis underestimates the glucose metabolic rate in normal liver, but that this further increases the contrast between tumour and liver and facilitates both tumour detection and quantification. Messa et al. concluded that this technique is computationally feasible and is well suited for serial evaluations of tumour metabolism during treatment. In our opinion, the technical improvements since that time facilitate such calculations and may introduce this technique into clinical oncological routine for both diagnosis and therapy management.

Non-compartmental approaches have been introduced, which have the advantage that no input function is needed. Such an approach is the calculation of the FD, a parameter based on the chaos theory^[12]. We used this approach on FDG time activity data and calculated parametric fractal images (Fig. 2). The calculation of FD images is reproducible, rapid, and operator independent. FD images can be calculated over time, as in Fig. 2, or over the space, in order to detect tissue heterogeneity in time. We applied this method to the time rather than the spatial axis. The noise of the curve may have an impact

on the calculation of FD in time. Therefore, we used 28 frames for the dynamic data acquisition in order to achieve a fine data sampling. Furthermore, for the VOI-based calculation of the FD, we used VOIs and not ROIs. Therefore, noise was not a major problem. Fractal images calculated in the spatial axis are more suitable for the evaluation of morphological images, such as CT or X-ray images, or even for evaluation of histology. Fractal images of bone CT scans or bone radiographs may be used to assess the trabecular structure^[16,17].

Short acquisition protocols are less time consuming and may find use in clinical routine. We demonstrated that in the case of FDG a short dynamic series of 16 min or a combination of short series and a late static image 60 min post injection is accurate for the prediction of the kinetic parameters of FDG. This approach is based on a database obtained in oncological patients in our department and a dedicated software package, which uses the SVM algorithm for prediction of the kinetic data. The best results have been reported for the calculation of V_B and k_1 using short acquisition protocols, whereas k_3 is the most critical parameter for prediction with the highest statistical noise^[13].

Conclusion

Quantitative, dynamic PET/CT imaging, including the calculation of parametric images, is a challenge, and will find its way into clinical routine. Technical improvements in the equipment, such as computer power, faster data acquisition by new-generation PET/CT scanners, with better detector material and the possibility to perform multi-bed dynamic imaging, as well as more sophisticated software for data evaluation, will facilitate this step.

References

- [1] Dimitrakopoulou-Strauss A, Strauss LG, Schwarzbach M, et al. Dynamic PET ¹⁸F-FDG studies in patients with primary and recurrent soft-tissue sarcomas: impact on diagnosis and correlation with grading. *J Nucl Med* 2001; 42: 713–720. PMID:11337565.
- [2] Dimitrakopoulou-Strauss A, Hoffmann M, Bergner R, et al. Prediction of short-term survival in patients with advanced nonsmall cell lung cancer following chemotherapy based on 2-deoxy-2-(F-18)-fluoro-D-glucose positron emission tomography: a feasibility study. *Mol Imaging Biol* 2007; 9: 308–317. doi:10.1007/s11307-007-0103-6. PMID:17623254.
- [3] Dimitrakopoulou-Strauss A, Hohenberger P, Pan L, Kasper B, Roumia S, Strauss LG. Dynamic PET (dPET) with FDG in patients with unresectable aggressive fibromatosis: regression-based parametric images and correlation to the FDG kinetics based on a two-tissue compartment mode. *Clin Nucl Med* 2012; in press. PMID:21220970.
- [4] Apostolopoulos DJ, Dimitrakopoulou-Strauss A, Hohenberger P, Roumia S, Strauss LG. Parametric images via dynamic ¹⁸F-fluorodeoxyglucose positron emission tomographic data acquisition in predicting midterm outcome of liver metastases secondary to gastrointestinal stromal tumours. *Eur J Nucl Med Mol Imaging* 2011; 38: 1212–223. doi:10.1007/s00259-011-1776-2. PMID:21400009.
- [5] Strauss LG, Conti PS. The applications of PET in clinical oncology. *J Nucl Med* 1991; 32: 623–648. PMID:2013803.
- [6] Mikolajczyk K, Szabatin M, Rudnicki P, Grodzki M, Burger C. A Java environment for medical image data analysis: initial application for brain PET quantitation. *Med Inform* 1998; 23: 207–214. doi:10.3109/14639239809001400.
- [7] Burger C, Buck A. Requirements and implementations of a flexible kinetic modeling tool. *J Nucl Med* 1997; 38: 1818–1823. PMID:9374364.
- [8] Patlak CS, Blasberg RG. Graphical evaluation of blood-to-brain transfer constants from multiple-time uptake data. Generalizations. *J Cereb Flow Metab* 1985; 5: 584–590. doi:10.1038/jcbfm.1985.87.
- [9] Ohtake T, Kosaka N, Watanabe T, et al. Noninvasive method to obtain input function for measuring glucose utilization of thoracic and abdominal organs. *J Nucl Med* 1991; 32: 1432–1438. PMID:2066802.
- [10] Miyazawa H, Osmont A, Petit-Taboue MC, et al. Determination of ¹⁸F-fluoro-2-deoxy-D-glucose rate constants in the anesthetized baboon brain with dynamic positron tomography. *J Neurosci Methods* 1993; 50: 263–272. doi:10.1016/0165-0270(93)90033-N. PMID:8152238.
- [11] Sokoloff L, Smith CB. Basic principles underlying radioisotopic methods for assay of biochemical processes in vivo. In: Greitz T, Ingvar DH, Widén L, editors. *The metabolism of the human brain studied with positron emission tomography*. New York: Raven Press; 1983, p. 123–148.
- [12] Dimitrakopoulou-Strauss A, Strauss LG, Burger C, et al. On the fractal nature of positron emission tomography (PET) studies. *World J Nucl Med* 2003; 4: 306–313.
- [13] Strauss LG, Pan L, Cheng C, Haberkorn U, Dimitrakopoulou-Strauss A. Shortened acquisition protocols for the quantitative assessment of the 2-tissue-compartment model using dynamic PET/CT ¹⁸F-FDG studies. *J Nucl Med* 2011; 52: 379–385. doi:10.2967/jnumed.110.079798. PMID:21321263.
- [14] Pan L, Mikolajczyk K, Strauss L, Haberkorn U, Dimitrakopoulou-Strauss A. Machine learning based parameter imaging and kinetic modeling of PET data. *J Nucl Med* 2007; 48: 158P.
- [15] Messa C, Choi Y, Hoh CK, Jakobs EL, et al. Quantification of glucose utilization in liver metastases: parametric imaging of FDG uptake with PET. *J Comput Assist Tomogr* 1992; 16: 684–689. doi:10.1097/00004728-199209000-00003. PMID:1522257.
- [16] Dougherty G. A comparison of the texture of computed tomography and projection radiography images of vertebral trabecular bone using fractal signature and lacunarity. *Med Eng Phys* 2001; 23: 313–321. doi:10.1016/S1350-4533(01)00048-0. PMID:11435145.
- [17] Oka K, Kumasaka S, Kashima I. Assessment of bone feature parameters from lumbar trabecular skeletal patterns using mathematical morphology image processing. *J Bone Miner Metab* 2002; 20: 201–208. doi:10.1007/s007740200029. PMID:12115065.